JOURNAL OF GEOPHYSICAL RESEARCH, VOL. ???, XXXX, DOI:10.1029/,

# Chapter 5: Gravity Waves in the Stratosphere

M. Joan Alexander[1]

M. J. Alexander, NWRA, Colorado Research Associates Div., 3380 Mitchell Lane, Boulder, CO 80301, USA.

[1] NWRA, Colorado Research Associates Div., 3380 Mitchell Lane, Boulder, CO 80301, USA.

**Abstract.** This chapter presents a review of some recent research highlighting direct gravity wave effects in the stratosphere. In the last 20 years, our understanding of the range of these effects has grown in tandem with improvements in resolution in both observations and models. The effects include gravity wave-driving of the general circulation, temperature structure and related effects on polar ozone chemistry, and effects on ice clouds. Recent observations of gravity waves in the stratosphere that help to quantify these effects are also highlighted. The observations are giving the picture of a collection of events, occurring sporadically in localized wave packets, superimposed on a weaker background spectrum of waves. Finally, new information on the sources of gravity waves gleaned from both the observations and wave-resolving models are also summarized. The improved knowledge of these sources is expected to lead to advances in gravity wave parameterizations in global climate models that will permit more realistic feedbacks between the waves and future climate change.

## 1. Introduction

Prior to 1987 when *Andrews et al.* [1987] was published, we had a clear understanding of the global effects of gravity waves in the mesosphere. A working parameterization of gravity wave forcing effects on the global circulation had been developed for global models [*Lindzen*, 1981; *Holton*, 1982, 1983], and the modeling community had also come to appreciate the effects of mountain wave drag near the tropopause on the general circulation and the importance of this process in both weather forecasting and climate models [*Palmer et al.*, 1986; *McFarlane*, 1987]. A successful theory for the forcing effects of wave dissipation on the mean flow had been developed, and was the cornerstone of these developments [*Andrews and Mc Intyre*, 1976; *Boyd*, 1976; *Andrews et al.*, 1987]. The transformed Eulerian-mean equations form the simplest equation set that describes both the direct effects of wave forcing on the zonal circulation as well as the effects on the meridional transport circulation and the temperature structure of the atmosphere. In their quasigeostrophic form derived on a beta plane, they are a simple set that will be useful for the discussion in this chapter. Reproducing equations 3.5.5 from *Andrews et al.* [1987],

$$\bar{u}_t - f_0\bar{v}^* = \bar{X} + \rho_0^{-1}\nabla \cdot \mathbf{F} \tag{1}$$

$$\bar{\theta}_t + \bar{w}^*\theta_{0z} = \bar{Q} \tag{2}$$

$$\bar{v}_y^* + \rho_0^{-1}(\rho_0\bar{w}^*)_z = 0 \tag{3}$$

The momentum ($\bar{X}+\nabla\cdot\mathbf{F}/\rho_0$) and thermal ($\bar{Q}$) forcing terms are placed on the right-hand sides. Here $(\bar{u}, \bar{v})$ is the zonal-mean wind, $\theta_0$ and $\rho_0$ are reference potential temperature and density that vary with height only, and $f_0$ the Coriolis parameter defined in the center of the beta plane. These equations describe the temperature and circulation responses to a wave-driven forcing. The momentum equation (1) shows that a driven momentum forcing can lead to both wind accelerations ($\bar{u}_t$) as well as meridional drift through the Coriolis torque ($f_0\bar{v}^*$). Via continuity (3), the meridional drift is associated with vertical motions ($\bar{w}^*$), which are tied to thermal changes via the thermodynamic equation (2). The meridional transport circulation is approximated here by the residual circulation ($\bar{v}^*, \bar{w}^*$) defined by

$$\bar{v}^* = \bar{v}_a - \rho_0^{-1}(\rho_0\overline{v'\theta'}/\theta_{0z})_z,$$

$$\bar{w}^* = \bar{w}_a + (\overline{v'\theta'}/\theta_{0z})_y. \quad (4)$$

In this quasi-geostrophic beta-plane case the divergence of the Elliassen-Palm flux has only two terms due to eddy momentum and heat fluxes, $\nabla \cdot \mathbf{F} = -(\rho_0\overline{v'u'})_y + (\rho_0 f_0\overline{v'\theta'}/\theta_{0z})_z$. The other momentum forcing term could be the forcing due to parameterized gravity waves and be written as the vertical gradient in wave stress or momentum flux $\bar{X} = -\rho_0^{-1}(\rho_0\overline{u'w'})_z$. In gravity wave parameterization schemes, the momentum flux $\rho_0\overline{u'w'}$ is specified at some altitude along with other wave propagation properties, and the parameterization determines the force $\bar{X}$. Mountain wave parameterizations treat only stationary waves, while "non-orographic" gravity wave parameterizations treat a broad spectrum of phase speeds.

*Holton and Alexander* [2000] reviewed the fundamentals of planetary waves and gravity waves, and their roles in driving the transport circulation of the middle atmosphere. In this chapter, we specifically highlight effects of gravity waves at stratospheric levels. Section 2 describes these effects, particularly those that have been discovered in recent decades. Many of these effects have been inferred from global model studies. Knowledge of gravity wave sources and momentum fluxes have been a limitation in quantifying these effects. Recent observations discussed in section 3 show that gravity wave momentum fluxes in the lower stratosphere can vary considerably in individual measurements and can be traced to specific wave sources. The measurements also show seasonal and latitudinal patterns that may begin to describe a climatology. Climate change may result in long term variations in gravity wave sources, so there is current interest in developing non-orographic source parameterizations for moist convection and jet stream sources that will respond to changing climate in the way mountain wave parameterizations currently do. The non-orographic parameterizations applied in today's chemistry-climate models do not change with changing climate, and this is a limitation in their use for forecasts. We therefore focus in section 4 on gravity wave sources.

## 2. Gravity wave effects in/on the stratosphere

In the last 20 years, there have been some notable developments in our understanding of gravity wave effects at stratosphere levels in contrast to the previous understanding of their effects at higher levels in the mesosphere. In the mesosphere, gravity waves have first-order effects. Their dissipation near the mesopause causes complete reversals in the direction of the zonal-mean winds, and the resulting pole-to-pole meridional circulation drives the temperature structure very far from radiative equilibrium. At the polar summer mesopause where the sun shines continously, but the wave-driven Lagrangian-mean meridional circulation (4) leads to upwelling, temperatures are the coldest found anywhere in the atmosphere. The polar winter mesopause, conversely in complete darkness, is relatively warm due to net downwelling. These upper atmosphere effects were discussed and illustrated in *Andrews et al.* [1987].

Gravity wave effects in the stratosphere, in contrast are second order. Planetary waves in the extratropics and global-scale equatorial waves account for the majority of the wave-driven circulation effects. However, recent developments have shown the importance of gravity waves. They serve as helpers, with their effects responding to and exaggerating changes in the winds initiated by the global-scale-wave driving. In some situations, gravity waves account for the majority of the wave driving effects. We next describe several notable examples of the direct effects of gravity waves on the circulation in the stratosphere.

### 2.1 Extratropical effects

#### 2.1.1 Wave driving of the Brewer-Dobson circulation.

The equator-to-pole Lagrangian-mean meridional transport circulation in the stratosphere is called the Brewer-Dobson circulation for researchers who first proposed it [*Brewer*, 1949; *Dobson*, 1956]. The circulation is largely driven by planetary wave drag [*Yulaeva et al.*, 1994], but the summer hemisphere branch and the seasonal variation in the strength of the circulation is linked to forcing from dissipation of smaller scale gravity waves that are not resolved in most global models and instead are treated via parameterization. *Alexander and Rosenlof* [2003] used observations to derive the seasonal cycle of net extratropical wave forcing across the 90.7 hPa surface in the lower stratosphere of each hemisphere using the solution for the residual circulation [*Rosenlof*, 1996] and the net wave-driven force $F$ required to balance the transformed Eulerian mean momentum equation. They then computed the resolved wave contribution to EP-flux divergence from a global analysis and by subtraction, the gravity wave (unresolved) forcing. Their results

(Figure 1) show that the resolved forcing drives the wintertime maximum in the Brewer-Dobson circulation in each hemisphere, but that smaller-scale gravity waves dominate the wave forcing in the spring-to-summer transition season in each hemisphere.

#### 2.1.2 Transition to summer easterlies.

Global circulation models that do not include parameterized non-orographic gravity waves tend to have trouble in describing the spring-to-summer transition of extratropical winds and temperatures in the stratosphere. The transition from winter eastward winds to summer westward winds tends to occur approximately a month too late. *Scaife et al.* [2002] demonstrated that this problem can be resolved using a parameterization of non-orographic gravity waves (Figure 2). A spectrum of westward propagating gravity waves with non-zero phase speeds is required to accelerate the winds and transition from eastward to westward. Orographic waves can only drag the winds towards zero but not accelerate them to westward values. The westward gravity wave forcing responsible for this will not only improve the timing of the transition from eastward to westward winds, but will also help to drive the summer-hemisphere cell of the Brewer-Dobson circulation.

#### 2.1.3 The cold-pole problem and ozone chemistry.

Global models without parameterized small-scale wave drag have stratospheric polar winter temperatures that are far colder than observed [*Palmer et al.*, 1986; *McFarlane*, 1987]. Resolved planetary wave drag is insufficient to drive the full strength of the winter residual circulation downwelling. Gravity wave drag at both stratospheric and mesospheric levels are important to accurate modeling of stratospheric temperatures [*Garcia and Boville*, 1994]. Some of the required drag is provided via mountain wave parameterizations [*Boville*, 1991]. Spectral gravity wave parameterizations provide additional drag at winter polar latitudes that is particularly important in the southern hemisphere winter. Climate simulations designed to predict future ozone changes, so-called “chemistry-climate models,” require some form of gravity wave parameterization, which has the effect of adjusting stratospheric polar winter temperatures to more realistic values, before temperature sensitive chemical reactions can be accurately modeled [*Austin et al.*, 2003; *Eyring et al.*, 2007].

### 2.1.4 Polar stratospheric clouds and ozone chemistry.

Polar stratospheric clouds (PSCs) form as winter stratospheric temperatures drop below 195K. Chemical reactions on the surfaces of these PSCs convert reservoir chlorine species into chemically active forms that destroy ozone when sunlight returns in spring. The clouds may also denitrify polar air, inhibiting reactions that convert the active chlorine back to the reservoir forms [*Solomon and Schoeberl*, 1988; *Tolbert and Toon*, 2001]. Northern hemisphere winter polar temperatures are warmer than those in the southern hemisphere, and correspondingly PSCs are more widespread and persistent in the south. These differences in PSC occurrence are a primary reason for hemispheric differences in seasonal ozone loss. High latitude mountain waves cause temperature perturbations, and PSCs have been observed to form in the cold phases of the waves in conditions that are otherwise too warm [*Dörnbrack et al.*, 2002]. The chemistry occurring on the surfaces of these clouds is not reversed when the air parcel subsequently passes through the adjacent warm phase of the wave. So net chlorine activation results, and the absence of these small-scale wave features may account for underprediction of Arctic ozone depletion in some models [*Carslaw et al.*, 1998]. Wave-induced clouds may also affect ozone abundance in the Arctic and Antarctic through denitrification following the formation and sedimentation of PSCs [*Mann et al.*, 2005; *Höpfner et al.*, 2006; *Eckermann et al.*, 2009]. (See Figure 3.)

## 2.2 Tropical effects

### 2.2.1 Gravity wave forcing of the QBO.

Twenty years ago, the quasibiennial oscillation (QBO) in stratospheric zonal winds was understood to be driven by dissipation of tropical waves, but a quantitative working model of the QBO remained elusive. The primary wave forcing was believed to come from eastward propagating Kelvin waves and westward propagating mixed-Rossby-gravity waves [*Holton and Lindzen*, 1972], and the mechanism further elucidated by *Plumb* [1977]. These equatorial wave mechanisms supplanted an earlier theory for gravity wave driving [*Lindzen and Holton*, 1968]. It is now known that a broad spectrum of waves in the tropics contribute to the forcing of the QBO, including both equatorial wave modes and higher frequency gravity waves [*Dunkerton*, 1997; *Sato and Dunkerton*, 1997]. Reproducing the phenomenon in a 3-dimensional global model requires high vertical (0.5-0.75 km) to simulate the resolved wave and mean-flow interaction [*Baldwin et al.*, 2001; *Hamilton*, 2008]. Realistic simulations at zonal resolutions near 4° have additionally required parameterization of the effects of small-scale gravity waves [*Giorgetta et al.*, 2002; *Scaife et al.*, 2002] as well as use of a convective parameterization that reproduces high-frequency variability in convection that results in a broad spectrum of resolved waves [*Takahashi*, 1996; *Ricciardulli and Garcia*, 2000; *Horinouchi et al.*, 2003]. Recent model studies suggest that small-scale gravity waves provide roughly half of the eastward propagating wave flux and half or possibly much more of the westward propagating wave flux needed to drive the QBO [*Giorgetta et al.*, 2002; *Scaife et al.*, 2000; *Kawatani et al.*, 2009], with the gravity waves contributing relatively more in the upper stratosphere and the resolved waves more in the lower stratosphere.

### 2.2.2 Gravity wave forcing of the stratopause semiannual oscillation.

The semiannual oscillation (SAO) in zonal winds near the stratopause is driven by a combination of processes. The westward phases are in part due to the advection of summer westward winds across the equator by the residual circulation. Additional forcing comes from wave dissipation, likely including Kelvin, Rossby, Rossby-gravity, and gravity waves [*Hitchman and Leovy*, 1988; *Sassi and Garcia*, 1997; *Garcia et al.*, 1997; *Ray et al.*, 1998].

Small scale gravity waves may play a relatively important role in descent of the eastward phases [*Garcia et al.*, 1997; *Ray et al.*, 1998]. This conclusion follows from: (1) the observation that the eastward phase descent is asymmetric about the equator indicating a lesser role for planetary scale Kelvin waves, which are symmetric; (2) the fact that underlying QBO eastward winds are much weaker than their westward counterparts and will therefore filter a smaller fraction of the upward propagating wave spectrum that reaches the upper stratosphere to drive the SAO.

### 2.2.3 Tropical cirrus.

Waves of all scales can modulate or initiate the formation of cirrus clouds near the tropical tropopause in the cold phases of the waves. The wave amplitude can determine ice cloud formation when air is otherwise too warm, and the cooling rate (related to the wave intrinsic frequency) will influence ice particle sizes, number densities, and sedimentation.

When ice particles grow large enough to fall, this further affects water vapor concentrations. If the waves affect water vapor near the tropical tropopause in this way, they may thus play a role in the dehydration of air entering the tropical stratosphere, which is subsequently transported globally via the stratospheric residual circulation. Waves may thus influence stratospheric dehydration, cirrus cloud occurrence frequencies, cirrus optical depth, and cloud radiative properties.

Observations have shown that Kelvin waves influence cirrus cloud formation [*Boehm and Verlinde*, 2000; *Fujiwara et al.*, 2009]. The effects of gravity waves in the above processes are poorly understood at present, but model studies indicate a potentially important role for gravity waves in determining cirrus cloud occurrence frequencies [*Jensen and Pfister*, 2004], and particle sizes [*Jensen et al.*, 2009].

### 2.3 The role of gravity waves in model responses to climate change

#### 2.3.1 Mountain wave parameterization effects on the climate response to increasing $CO_2$.

Sigmond et al. [2008][*Sigmond et al.*, 2008] examined differences in the atmospheric circulation response to $CO_2$ doubling in two models: one designed for climate forecasts, and the other designed for chemistry-climate forecasts. The latter is distinguished by a well resolved stratosphere, but the two models also include different tunings due to the different purposes for which they were designed. The authors show substantially different northern hemisphere winter surface pressure response patterns in the two models, and investigate possible causes of the differences. The responses were not very sensitive to the differences in stratospheric resolution or the level of the model top. Instead, differences in the orographic gravity wave parameterizations explained most of the differences in the surface pressure response pattern. Specifically, a parameter that describes the momentum flux of the orographic waves when given identical settings in the two models brought the models into much closer agreement. Larger flux settings cause larger wave drag and weaker winds in the lowermost stratosphere, which in turn affect planetary wave propagation into the stratosphere that leads to changes in surface pressure patterns. The result underscores how uncertainty in mountain wave parameterization settings can influence climate response patterns.

### 2.3.2 Trends in the Brewer-Dobson circulation.

Chemistry-climate models require a well-resolved middle atmosphere. Recent model intercomparisons describe increased upwelling across the tropical tropopause and increases in the Brewer-Dobson transport circulation as robust features of the model responses to $CO_2$ increases [*Butchart et al.*, 2006]. The cause of the transport circulation increases must be related to changes in stratospheric wave forcing, because stratospheric wave dissipation drives the transport circulation. However, the changes in wave dissipation need not be related to changes in wave fluxes from the troposphere. Instead, the wave dissipation may simply change due to changes in winds and stability in the stratosphere. The relative contributions of these two factors is not yet known.

Chemistry-climate models include realistic scenarios for increasing greenhouse gases in the 21st century. All climate models show that increasing greenhouse gases result in both tropospheric warming as well as stratospheric cooling. These changes are in turn associated with an increased latitudinal temperature gradient in the subtropical upper troposphere/lower stratosphere, which in turn is related to increases in the subtropical jet strength at upper levels. The wind response to changes in the temperature gradient is easily understood from geostrophic balance.

Several recent studies address the question of which waves are responsible for the future trends in the tropical upwelling in chemistry-climate models. Planetary waves, orographic gravity waves, and equatorial waves likely all contribute to the changes to some degree, but different model analyses have come to slightly different conclusions. Two recent studies found that changes in parameterized orographic wave drag were important in explaining the upwelling trends [*Li et al.*, 2008; *McLandress and Shepherd*, 2009]. Subtropical orographic wave drag shifts to higher altitudes in the future climate in response to increases in the winds in the lowermost stratosphere in these models. Planetary-scale waves are also important to explaining the trends, but the small- and large-scale waves may be most important at somewhat higher and lower altitudes respectively [*McLandress and Shepherd*, 2009]. (See Figure 4.) *McLandress and Shepherd* [2009] further showed that these conclusions can be very sensitive to the range of tropical latitudes included in the diagnosis of the trends in tropical upwelling, and that this sensitivity may account for apparently different conclusions about the type of waves responsible drawn by *Li et al.* [2008] and *Garcia and Randel* [2008].

## 3. Observations of Gravity Wave Momentum Flux

Many of the issues described above are treated via parameterization of gravity wave mean-flow forcing effects. These parameterizations require specification of the wave stress or momentum flux at the locations of wave sources (for mountain waves) or as a function of latitude at some arbitrary level near tropopause (for non-orographic gravity waves). Observational constraints on these fluxes have been lagging behind the application of the parameterizations in global models. Mountain wave parameterizations were employed in all but one of the climate models that participated in the last IPCC AR4 report [*Solomon et al.*, 2007]. The parameterizations are also widely used in global weather forecasting assimilation systems particularly the widely used products of the European (ECMWF) and US (NCEP) operational forecast centers. Non-orographic gravity wave parameterizations were an indispensable component in each of the set of models used for ozone chemistry-climate forecasts for the last ozone assessment. (See WMO/UNEP, [2007] and more indepth analyses described in *Eyring et al.* [2007]). As mentioned above (sec. 2.1.3), these non-orographic wave parameterizations were needed to tune the polar circulation and subsequent effects on polar winter temperatures in order to describe realistic chemical changes in the models [*Austin et al.*, 2003]. Without the gravity wave parameterizations, the polar winter temperatures are far too cold, and this leads to serious errors in the temperature-sensitive ozone chemistry in these models. The modelers could tune the gravity wave schemes to adjust these winter polar temperatures to reasonable values that allowed realistic hindcasts and forecasts of ozone changes and recovery.

The key uncertain parameter in these gravity wave schemes is the wave stress or momentum flux. The research community looked to observations to constrain these fluxes and to give guidance on how they might vary with latitude and season. Global data sets were needed. Satellites could provide the needed coverage, and improvements in resolution of satellite measurements meant that they began to resolve gravity waves in the 1990s [*Fetzer and Gille*, 1994; *Wu and Waters*, 1996]. However, these measurements provided only temperature variance and potential energy, whereas the gravity wave schemes require constraints on momentum flux. Early theories of the wave spectrum predicted that the potential energy distributions could be used as a proxy for momentum flux [*Fritts and VanZandt*, 1993], however mounting observational evidence called these assumptions in the spectral theory into question. Patterns in satellite maps of gravity wave potential energy were further noted to be highly dependent on the portion of the wave spectrum visible to each satellite instrument [*Alexander*, 1998; *Preusse et al.*, 2008].

Long-duration quasi-Lagrangian balloon flights in the lower stratosphere have provided some of the most accurate measurements of gravity wave momentum fluxes and their direction. Vector momentum fluxes from one of these balloon campaigns is shown in Figure 5. Regional variations tied to mountain wave sources are apparent. A high degree of intermittency in wave was also observed and quantified from these data [*Hertzog et al.*, 2008].

Recent high resolution satellite observations of gravity wave temperature fluctuations have been used to produce global maps of momentum flux computed directly from the observations at altitudes in the lower stratosphere [*Ern et al.*, 2004; *Alexander et al.*, 2008]. These momentum flux calculations require simultaneous measurement of the three-dimensional wave structure (both horizontal and vertical wavelength) to convert the observed wave temperature amplitudes to momentum fluxes. (See Figure 6.) The global momentum fluxes so far determined this way have lacked information on the wave propagation direction. This limitation renders the estimates of horizontal wavelength uncertain, and it leaves the estimates of momentum flux uncertain to the same degree. Despite these uncertainties, certain patterns emerge:

• Average horizontal wavelengths tend to be much longer in the equatorial region than at higher latitudes. This result agrees with analyses of radiosonde data [*Wang et al.*, 2005].

• Because of the horizontal wavelength trend, potential energy maps show weaker latitudinal gradients than momentum flux maps in side-by-side comparisons, a result that confirms that wave potential energy measurements alone cannot be used quantitatively to constrain momentum flux.

• Wave momentum fluxes are generally much larger in winter seasons than in summer.

• Large amplitude mountain waves have been identified, and large average fluxes appear where notable mountain wave sources occur, such as over the Andes and Antartic peninsula.

• A high degree of day-to-day variability has been observed (also called intermittency), a result also quantified in analyses of super-pressure balloon data [*Hertzog et al.*, 2008].

Some cautionary statements are needed along with the presentation of these general results:

• Although the satellite measurements used to estimate momentum fluxes are sensitive to a broad range of vertical wavelengths, some observational filtering associated with the analysis methods are likely to still affect the global patterns observed to some degree.

• The noise and other limits in sensitivity of the measurements will mean that weak waves in the stratosphere will not be observed, and these results therefore focus on larger-amplitude events. This could limit the applicability of these observational constraints on gravity wave forcing in the mesosphere and lower thermosphere, because very weak waves occurring in the stratosphere can still grow to large amplitudes before reaching the mesopause. Therefore, weak waves that are either not observed or not emphasized in the existing satellite results might still have profound effects near the mesopause.

- The satellite analyses assume that the waves observed are propagating upwards from sources below. Wave breaking events can induce secondary wave emission [*Holton and Alexander*, 1999; *Satomura and Sato*, 1999; *Vadas et al.*, 2003], generating waves that propagate both upwards and downwards. The prevalence or rarity of this process is not currently known. Because wave amplitudes increase with height due to the exponential decrease in density with height, these secondary waves may be far more prominent at higher altitudes, one indication that nonlinear processes become more important in shaping the gravity wave spectrum at mesospheric altitudes. Approximately linear propagation from identifiable tropospheric sources is more common at stratospheric altitudes.

## 4. Sources and Wave Generation Mechanisms

Section 2 summarized some of the ways that gravity wave processes can affect climate forecast models. These processes are treated via parameterization in global climate and chemistry-climate models. The computational demands for such forecasts across century or longer timescales will likely keep model vertical and horizontal resolution too coarse into the near future to model gravity wave process directly, so the parameterizations will continue to be needed. Current operational versions of the climate models include mountain wave parameterizations that will respond to some degree to climate change. Changes in surface wind and stability will change the waves generated by orography, and thus mountain wave source parameterizations have some prognostic capability.

If considered at all, gravity waves from other sources are usually given properties that do not vary with time and may vary only gradually with latitude in operational models.

These non-orographic wave parameterizations are a particularly important component of chemistry-climate models, and the sources for the waves modeled in this way are meant to include convection, various processes active in the jet stream like frontal development and jet imbalance, and others (see *e.g. Fritts and Alexander* [2003]). Wave source parameterizations for fronts [*Charron and Manzini*, 2002] and convection [*Chun et al.*, 2004; *Beres et al.*, 2005] have been proposed and implemented in research versions of climate models, but the parameterizations are poorly validated against observations at present. High-resolution theoretical model studies have examined waves emanating from these sources and also from regions of jet imbalance. Below we briefly summarize some recent results from high-resolution model studies of convection and jet sources.

### 4.1 Waves generated by convection.

Latent heating within convection is a source for waves because it is localized and time-dependent. In the absence of wind shear, the duration and scale of the heating roughly describe lower limits on the wave period and wavelength that can be generated. So intense, short-duration, small-scale heating events are efficient wave sources over a broad range of gravity wave properties.

Convection can in general generate a broad spectrum of wave phase speeds, with peaks in the stratospheric spectrum above the storm related to the depth of the heating within the storm [*Alexander et al.*, 1995; *Piani et al.*, 2000; *Beres et al.*, 2002; *Holton et al.*, 2001].

A separate peak in the spectrum at a phase speed approximately matching the motions of the heating cells within the storm also appears when there is upper level shear or when the wind near the top of the heating cell is at least $\sim$5 m/s relative to the heating cell motion [*Pfister et al.*, 1993; *Beres et al.*, 2004; *Alexander et al.*, 2006; *Kuester et al.*, 2008]. (See Figure 7.) This wind-sensitive peak is associated with waves generated by the so-called "obstacle effect", a mechanism analogous to orographic wave generation [*Chun and Baik*, 1998].

Additional spectral peaks may be associated with oscillations within the storm at specific frequencies [*Fovell et al.*, 1992; *Alexander et al.*, 1995]. *Lane and Reeder* [2001] proposed the "oscillator" could be described as moist air parcels rising to their level of neutral buoyancy and oscillating there at the local moist buoyancy frequency. This implies waves from this source would be associated with very high frequencies, those with frequencies characterized by buoyancy frequencies that occur in the upper troposphere.

One recent model study of waves generated by convection has been validated by comparison to observation from the AIRS satellite [*Grimsdell et al.*, 2009].

### 4.2 Waves from jet sources.

Models of waves generated by jet sources are apparently sensitive to model resolution [*O'Sullivan and Dunkerton*, 1995; *Zhang*, 2004] because such models require both high resolution and large domain sizes. (See Figure 8.) Analysis of the waves in these models is complicated by the complexities of the wind field in the vicinity of the wave source [*Plougonven and Snyder*, 2005; *Bühler and McIntyre*, 2005]. Strong horizontal and vertical gradients in the winds lead to dramatic changes in the observed wave spectrum through processes like wave refraction, critical level filtering, trapping, and preferential propagation. These can all have dramatic effects on the spectrum, making it very difficult to isolate the spectrum emanating from the source and difficult to develop a parameterization for waves from this source. Validation of a model of waves from jet sources by comparison to satellite observation appears in *Wu and Zhang* [2004].

## 5. Summary

In the last 20 years our understanding of the range of gravity wave effects in the stratosphere has grown in tandem with improved resolution in both observations and models. The direct effects of gravity waves in the stratosphere are numerous and significant, but generally smaller in magnitude than the effects of planetary-scale waves. Treatment of gravity wave effects on the circulation via parameterization has become standard practice in global climate and weather forecasting models.

A lack of observational constraints for parameterizations of gravity wave circulation effects in global models has limited our quantitative understanding of these effects. Recent satellite observations have sufficient resolution to provide some global constraints. Global constraints on momentum fluxes and wave propagation properties are needed. The observations give a picture of the waves as a collection of events in the stratosphere, sporadically occurring in very localized wave packets, probably superimposed upon a weaker background wave field.

High-resolution models with observational validation are giving us a clearer understanding of gravity wave sources and mechanisms, which is expected to lead to improved wave source parameterizations for global models. Existing parameterizations for mountain wave sources and future parameterizations for convection and jet sources will improve the prognostic capability of parameterizations of gravity wave circulation effects. These will permit more realistic feedbacks between future changes in climate and gravity waves in global models.

**Acknowledgments.** Supported by NASA Earth Science Division contract # NNH08CD37C and NSF Physical and Dynamic Meteorology Program grant # ATM-0632378.

## References

Alexander, M. J. (1998), Interpretations of observed climatological patterns in stratospheric gravity wave variance, *J. Geophys. Res.*, *103*, 8627–8640.

Alexander, M. J., and K. H. Rosenlof (2003), Gravity wave forcing in the stratosphere: Observational constraints from UARS and implications for parameterization in global models, *J. Geophys. Res.*, *108*(D19), doi:10.1029/2003JD003,373.

Alexander, M. J., J. R. Holton, and D. R. Durran (1995), The gravity wave response above deep convection in a squall line simulation, *J. Atmos. Sci.*, *52*, 2212–2226.

Alexander, M. J., J. H. Richter, and B. R. Sutherland (2006), Generation and trapping of gravity waves from convection, with comparison to parameterization, *J. Atmos. Sci.*, *63*(11), 2963–2977.

Alexander, M. J., et al. (2008), Global estimates of gravity wave momentum flux from High Resolution Dynamics Limb Sounder (HIRDLS) observations, *J. Geophys. Res.*, *113*(D15S18), doi:10.1029/2007JD008,807.

Andrews, D., J. Holton, and C. Leovy (1987), *Middle Atmosphere Dynamics*, 489 pp. pp., Academic Press, Orlando.

Andrews, D. G., and M. E. Mc Intyre (1976), Planetary waves in horizontal and vertical shear: The generalized Eliassen-Palm relation and the mean zonal acceleration, *J. Atmos. Sci.*, *33*, 2031–2048.

Austin, J., et al. (2003), Uncertainties and assessments of chemistry-climate models of the stratosphere, *Atmos. Chem. Phys.*, *3*, 1–27.

Baldwin, M. P., et al. (2001), The quasi-biennial oscillation, *Rev. Geophys.*, *39*, 179–229.

Beres, J., M. J. Alexander, and J. R. Holton (2004), A method of specifying the gravity wave spectrum above convection based on latent heating properties and background wind, *J. Atmos. Sci.*, *61*, 324–337.

Beres, J., R. Garcia, B. Boville, and F. Sassi (2005), Implementation of a gravity wave source spectrum parameterization dependent on the properties of convection in the Whole Atmosphere Community Climate Model (WACCM), *J. Geophys. Res.*, *110*(D10108), doi:10.1029/2004JD005,504.

Beres, J. H., M. J. Alexander, and J. R. Holton (2002), Effects of tropospheric wind shear on the spectrum of convectively generated gravity waves, *J. Atmos. Sci.*, *59*, 1805–1824.

Boehm, M., and J. Verlinde (2000), Stratospheric influence on upper tropospheric tropical cirrus, *Geophys. Res. Lett.*, *27*(19), 3209–3212.

Boville, B. A. (1991), Sensitivity of simulated climate to model resolution, *J. Climate*, *4*, 469–485.

Boyd, J. P. (1976), The noninteraction of waves with the zonally averaged flow on a spherical Earth and the interrelationships of eddy fluxes of energy, heat and momentum, *J. Atmos. Sci.*, *33*, 2285–.

Brewer, A. (1949), Evidence for a world circulation provided by the measurements of helium and water vapor distribution in the stratosphere, *Q. J. R. Meteorol. Soc.*, *75*, 351–363.

Bühler, O., and M. McIntyre (2005), Wave capture and wave-vortex duality, *J. Fluid Mech.*, *534*, 67–95.

Butchart, N., et al. (2006), Simulations of anthropogenic change in the strength of the Brewer-Dobson circulation, *Clim. Dyn.*, *27*, 727–741.

Carslaw, K. S., et al. (1998), Increased stratospheric ozone depletion due to mountain-induced atmospheric waves, *Nature*, *391*, 675–678.

Charron, M., and E. Manzini (2002), Gravity waves from fronts: Parameterization and middle atmosphere response in a general circulation model, *J. Atmos. Sci.*, *59*, 923–941.

Chun, H.-Y., and J.-J. Baik (1998), Momentum flux by thermally induced internal gravity waves and its approximation for large-scale models, *J. Atmos. Sci.*, *55*, 3299–3310.

Chun, H.-Y., I.-S. Song, J.-J. Baik, and Y.-J. Kim (2004), Impact of a convectively forced gravity wave parameterization in NCAR CCM3, *J. Climate*, *17*(18), 3530–3547.

Dobson, G. M. B. (1956), Origin and distribution of the polyatomic molecules in the atmosphere, *Proc. R. Soc. Lond.*, *236A*, 187–193.

Dörnbrack, A., T. Birner, A. Fix, H. Flentje, A. Meister, H. Schmid, E. V. Browell, and M. J. Mahoney (2002), Evidence for inertia-gravity waves forming polar stratospheric clouds over Scandinavia, *J. Geophys. Res.*, *107*(8287), doi:10.1029/2001JD000,452.

Dunkerton, T. (1997), The role of gravity waves in the quasi-biennial oscillation, *J. Geophys. Res.*, *102*, 26,053–26,076.

Eckermann, S. D., L. Hoffmann, M. Höpfner, D. L. Wu, and M. J. Alexander (2009), Antarctic NAT PSC belt of June 2003: Observational validation of the mountain wave seeding hypothesis, *Geophys. Res. Lett.*, *36*(L02807), doi:10.1029/2008GL036,629.

Ern, M., P. Preusse, M. J. Alexander, and C. D. Warner (2004), Absolute values of gravity wave momentum flux derived from satellite data, *J. Geophys. Res.*, *109*(D20103), doi:10.1029/2004JD004,752.

Eyring, V., et al. (2007), Multimodel projections of stratospheric ozone in the 21st Century, *J. Geophys. Res.*, *112*(D16303), doi:10.1029/2006JD008,332.

Fetzer, E. J., and J. C. Gille (1994), Gravity wave variance in LIMS temperatures. Part I: Variability and comparison with background winds, *J. Atmos. Sci.*, *51*, 2461–2483.

Fovell, R., D. Durran, and J. R. Holton (1992), Numerical simulations of convectively generated stratospheric gravity waves, *J. Atmos. Sci.*, *49*, 1427–1442.

Fritts, D. C., and M. J. Alexander (2003), A review of gravity wave dynamics and effects on the middle atmosphere, *Rev. Geophys.*, *41*(1), doi:10.1029/2001RG000,106.

Fritts, D. C., and T. E. VanZandt (1993), Spectral estimates of gravity wave energy and momentum fluxes, I: Energy dissipation, acceleration, and constraints, *J. Atmos. Sci.*, *50*, 3685–3694.

Fujiwara, M., et al. (2009), Cirrus observations in the tropical tropopause layer over the Western Pacific, *J. Geophys. Res.*, *114*(D09304), doi:10.1029/2008JD011,040.

Garcia, R., T. Dunkerton, R. Lieberman, and R. Vincent (1997), Climatology of the semiannual oscillation of the tropical middle atmosphere, *J. Geophys. Res.*, *102*, 26,019–26,032.

Garcia, R. R., and B. A. Boville (1994), "Downward control" of the mean meridional circulation and temperature distribution of the polar winter stratosphere, *J. Atmos. Sci.*, *51*, 2238–2245.

Garcia, R. R., and W. J. Randel (2008), Acceleration of the Brewer-Dobson circulation due to increases in greenhouse gases, *J. Atmos. Sci.*, *65*, 2731–2739.

Giorgetta, M. A., E. Manzini, and E. Roeckner (2002), Forcing of the quasi-biennial oscillation from a broad spectrum of atmospheric waves, *Geophys. Res. Lett.*, *29*(8), 86–1 to 86–4.

Grimsdell, A. W., M. J. Alexander, P. May, and L. Hoffmann (2009), Model study of waves generated by convection with direct validation via satellite, *J. Atmos. Sci.*, *66*, (accepted).

Hamilton, K. (2008), *Numerical Resolution and Modeling of the Global Atmospheric Circulation: A Review of Our Current Understanding and Outstanding Issues*, chap. 1, pp. 8–27, Springer Publishing.

Haynes, P. H., C. J. Marks, M. E. McIntyre, T. G. Shepherd, and K. P. Shine (1991), On the "downward control" of extratropical diabatic circulations by eddy-induced mean zonal forces, *J. Atmos. Sci.*, *48*, 651–678.

Hertzog, A., G. Boccara, R. A. Vincent, F. Vial, and P. Cocquerez (2008), Estimation of gravity wave momentum flux and phase speeds from quasi-lagrangian stratospheric balloon flights. Part II: Results from the Vorcore campaign in Antarctica, *J. Atmos. Sci.*, *65*(DOI: 10.1175/2008JAS2710.1), 3056–3070.

Hitchman, M. H., and C. B. Leovy (1988), Estimation of the Kelvin wave contribution to the semiannual oscillation, *J. Atmos. Sci.*, *45*, 1462–1475.

Holton, J. (1982), The role of gravity wave induced drag and diffusion in the momentum budget of the mesosphere, *J. Atmos. Sci.*, *39*, 791–799.

Holton, J., and M. Alexander (1999), Gravity waves in the mesosphere generated by tropospheric convection, *Tellus*, *51A-B*, 45–58.

Holton, J., and M. Alexander (2000), The role of waves in the transport circulation of the middle atmosphere, in *Atmospheric Science Across the Stratopause*, edited by D. Siskind, E. Eckermann, and M. Summers, pp. 21–35, AGU monograph.

Holton, J., M. Alexander, and M. Boehm (2001), Evidence for short vertical wavelength Kelvin waves in the DOE-ARM Nauru99 radiosonde data, *J. Geophys. Res.*, *106*, 20,125–20,129.

Holton, J. R. (1983), The influence of gravity wave breaking on the general circulation of the middle atmosphere, *J. Atmos. Sci.*, *40*, 2497–2507.

Holton, J. R., and R. S. Lindzen (1972), An updated theory for the quasi-biennial cycle of the tropical stratosphere, *J. Atmos. Sci.*, *29*, 1076–1080.

Höpfner, M., et al. (2006), MIPAS detects Antarctic stratospheric belt of NAT PSCs caused by mountain waves, *Atmos. Chem. Phys.*, *6*, 1221–1230.

Horinouchi, T., et al. (2003), Tropical cumulus convection and upward-propagating waves in middle-atmospheric GCMs, *J. Atmos. Sci.*, *60*, 2765–2782.

Jensen, E., and L. Pfister (2004), Transport and freeze drying in the tropical tropopause layer, *J. Geophys. Res.*, *109*(D02207), 10.1029/2003JD004,022.

Jensen, E. J., et al. (2009), On the importance of small ice crystals in tropical anvil cirrus, *Atmos. Chem. Phys.*, *9*, 5519–5537.

Kawatani, Y., K. Sato, T. J. Dunkerton, S. Watanabe, S. Miyahara, and M. Takahashi (2009), The roles of equatorial trapped waves and three-dimensionally propagating gravity waves in driving the quasi-biennial oscillation. Part I: Zonal mean wave forcing, *J.*

*Atmos. Sci.*, p. (submitted).

Kuester, M., M. Alexander, and E. Ray (2008), A model study of gravity waves over hurricane Humberto (2001), *J. Atmos. Sci.*, *65*, 3231–3246.

Lane, T., and M. Reeder (2001), Modelling the generation of gravity waves by a Maritime Continent thunderstorm, *Q.J.R. Meteorol. Soc.*, *127*, 2705–2724.

Li, F., J. Austin, and J. Wilson (2008), The strength of the Brewer-Dobson circulation in a changing climate: Coupled chemistry-climate model simulations, *J. Clim.*, *21*(DOI: 10.1175/2007JCLI1663.1), 40–57.

Lindzen, R. S. (1981), Turbulence and stress owing to gravity wave and tidal breakdown, *J. Geophys. Res.*, *86*, 9707–9714.

Lindzen, R. S., and J. R. Holton (1968), A theory of the quasi-biennial oscillation, *J. Atmos. Sci.*, *25*, 1095–1107.

Mann, G. W., K. S. Carslaw, M. P. Chipperfield, and S. Davies (2005), Large nitric acid trihydrate particles and denitrification caused by mountain waves in the Arctic stratosphere, *J. Geophys. Res.*, *110*(D08202), doi:10.1029/2004JD005,271.

McFarlane, N. A. (1987), The effect of orographically excited gravity wave drag on the general circulation of the lower stratosphere and troposphere, *J. Atmos. Sci.*, *44*, 1775–1800.

McLandress, C., and T. G. Shepherd (2009), Simulated anthropogenic changes in the Brewer-Dobson circulation, including its extension to high latitudes, *J. Clim.*, *22*(DOI: 10.1175/2008JCLI2679.1), 1516–1540.

O'Sullivan, D., and T. Dunkerton (1995), Generation of inertia-gravity waves in a simulated life cycle of baroclinic instability, *J. Atmos. Sci.*, *52*(21), 3695–3716.

Palmer, T. N., G. J. Shutts, and R. Swinbank (1986), Alleviation of a systematic westerly bias in general circulation and numerical weather prediction models through an orographic gravity wave drag parameterization, *Q. J. R. Meteorol. Soc.*, *112*, 1001–1039.

Pfister, L., K. R. Chan, T. P. Bui, S. Bowen, M. Legg, B. Gary, K. Kelly, M. Proffitt, and W. Starr (1993), Gravity waves generated by a tropical cyclone during the STEP Tropical field program: A case study, *J. Geophys. Res.*, *98*, 8611–8638.

Piani, C., D. Durran, M. Alexander, and J. Holton (2000), A numerical study of three-dimensional gravity waves triggered by deep tropical convection and their role in the dynamics of the QBO, *J. Atmos. Sci.*, *57*(22), 3689–3702.

Plougonven, R., and C. Snyder (2005), Gravity waves excited by jets: Propagation versus generation, *Geophys. Res. Lett.*, *32*(L18802), doi:1029/2005GL023,730.

Plumb, R. A. (1977), The interaction of two internal waves with the mean flow: Implications for the theory of the quasi-biennial oscillation, *J. Atmos. Sci.*, *34*, 1847–1858.

Preusse, P., S. D. Eckermann, and E. M. (2008), Transparency of the atmosphere to short horizontal wavelength gravity waves, *J. Geophys. Res.*, *113*(D24104), doi:10.1029/2007JD009,682.

Ray, E., M. Alexander, and J. Holton (1998), An analysis of the structure and forcing of the equatorial semiannual oscillation in zonal wind, *J. Geophys. Res.*, *103*, 1759–1774.

Ricciardulli, L., and R. Garcia (2000), The excitation of equatorial waves by deep convection in the NCAR Community Climate Model (CCM3), *J. Atmos. Sci.*, *57*(21), 3461–3487.

Rosenlof, K. (1996), Summer hemisphere differences in temperature and transport in the lower stratosphere, *J. Geophys. Res.*, *101*, 19,129–19,136.

Sassi, F., and R. Garcia (1997), The role of equatorial waves forced by convection in the tropical semiannual oscillation, *J. Atmos. Sci.*, *54*, 1925–1942.

Sato, K., and T. Dunkerton (1997), Estimates of momentum flux associated with equatorial Kelvin and gravity waves, *J. Geophys. Res.*, *102*, 26,247–26,261.

Satomura, T., and K. Sato (1999), Secondary generation of gravity waves associated with the breaking of mountain waves, *J. Atmos. Sci.*, *56*(22), 3847–3858.

Scaife, A., N. Butchart, C. Warner, D. Stainforth, and W. Norton (2000), Realistic quasi-biennial oscillations in a simulation of the global climate, *Geophys. Res. Lett.*, *27*(21), 3481–3484.

Scaife, A., N. Butchart, C. Warner, and R. Swinbank (2002), Impact of a spectral gravity wave parameterization on the stratosphere in the Met Office Unified Model, *J. Atmos. Sci.*, *59*, 1473–1489.

Sigmond, M., J. F. Scinocca, and P. J. Kushner (2008), The impact of the stratosphere on tropospheric climate change, *Geophys. Res. Lett.*, *35*(L12706), doi:10.1029/2008GL033,573.

Solomon, S., and M. R. Schoeberl (1988), Overview of the polar ozone issue, *Geophys. Res. Lett.*, *15*(8), 845–846.

Solomon, S., D. Qin, M. Manning, Z. Chen, M. Marquis, K. Averyt, M. Tignor, and H. L. Miller (Eds.) (2007), *IPCC, 2007: Climate Change 2007 - The Physical Science Basis: Contribution of Working Group I to the Fourth Assessment Report of the IPCC*, 996 pp. pp., Cambridge Univ. Press, Cambridge, UK and New York, NY, USA.

Takahashi, M. (1996), Simulation of the stratospheric quasi-biennial oscillation using a general circulation model, *Geophys. Res. Lett.*, *23*(6), 661–664.

Tolbert, M. A., and O. B. Toon (2001), Solving the PSC mystery, *Science*, *292*(5514), 61–63.

Vadas, S., D. Fritts, and M. Alexander (2003), Mechanism for the generation of secondary waves in wave breaking regions, *J. Atmos. Sci.*, *60*, 194–214.

Wang, L., M. A. Geller, and M. J. Alexander (2005), Spatial and temporal variations of gravity wave parameters. Part 1: Intrinsic frequency, wavelength, and vertical propagation direction, *J. Atmos. Sci.*, *62*, 125–142.

Wu, D. L., and J. W. Waters (1996), Gravity-wave-scale temperature fluctuations seen by the UARS MLS, *Geophys. Res. Lett.*, *23*(23), 3289–3292.

Wu, D. L., and F. Zhang (2004), A study of mesoscale gravity waves over the North Atlantic with satellite observations and a mesoscale model, *J. Geophys. Res.*, *109*(D22104), doi:10.1029/2004JD005,090.

Yulaeva, E., J. R. Holton, and J. M. Wallace (1994), On the cause of the annual cycle in the tropical lower stratospheric temperature, *J. Atmos. Sci.*, *51*, 169–174.

Zhang, F. (2004), Generation of mesoscale gravity waves in upper-tropospheric jet-front systems, *J. Atmos. Sci.*, *61*(4), 440–457.

**Figure 1.** Seasonal variations in downward mass flux at 90 hPa in the northern (NH) and southern (SH) hemispheres. The dashed and dotted curves show contributions from resolved planetary waves ($D_{EP}$) and unresolved gravity waves ($D_X$) derived from the two components of the wave-driven force and downward control at the latitude marking the poleward edge of tropical upwelling in each hemisphere. (After *Alexander and Rosenlof* [2003].)

**Figure 2.** Timing of the onset of westward winds near 60S latitude as a function of pressure through the spring-to-summer season in the UK Met Office model. "Assm" shows the result after assimilation of observations, and "No drag" is the free-running model without the parameterization of gravity wave forcing. "USSP" shows the improvement in the model timing with parameterized gravity wave drag. (After *Scaife et al.* [2002].)

**Figure 3.** Schematic showing the role of mountain wave temperature anomalies in denitrification of stratospheric air. The mountain waves (via a Mountain Wave Forecast Model (MWFM)) initiate formation of nitric acid trihydrate (NAT) clouds, followed by NAT particle growth and sedimentation of NAT "rocks" (larger particles) downstream. (After *Mann et al.* [2005].)

**Figure 4.** Analysis of NH chemistry-climate model results showing (a) distribution of mountain wave drag in the "past", (b) change in the mountain wave drag in the "future", (c) zonal mean winds in the "past" and (d) change in the zonal mean winds in the "future". "Past" here is the average in years 1960-1979, and "future" is the average 2080-2099. (After *McLandress and Shepherd* [2009].)

**Figure 5.** Zonal (left) and meridional (right) components of vector momentum flux derived from long-duration balloon flights in the southern lower stratosphere during September 2005 - Feb 2006. Large values over the Antarctic peninsula are associated with mountain waves. Too few measurements were made in hatched regions for a determination. (After *Hertzog et al.* [2008].)

**Figure 6.** Global maps of wave parameters, averaged over the 2005-6 winter season (Dec-Feb) at 20-30 km altitude. Clockwise from top left: Temperature amplitude, momentum flux, vertical wavelength, horizontal wavelength. Note the fluxes are lower limits (and horizontal wavelengths upper limits) because of the unknown wave propagation directions and associated errors in horizontal wavelengths. (Derived with analysis methods described in *Alexander et al.* [2008].)

**Figure 7.** Momentum flux versus phase speed and propagation direction (left panels) computed for waves in the stratosphere above convection with two different wind profiles (right). Top panels: The case with strong winds near the top of the convective heating. A peak in momentum flux occurs at phase speeds 0-10 m/s with northeastward (NE) propagation directions that is absent in the case without wind shear (bottom). These NE propagating waves match the motions of latent heating cells within the storm, marking the signature of the "obstacle effect" wave generation mechanism. (After *Alexander et al.* [2006].)

**Figure 8.** Four panels show a time series of waves emitted by a jet-front system in a model study at 13-km altitude. Thin dashed and solid contours show wind divergence, and thick contours show isobars. Wind vectors are also shown. (After *Zhang* [2004].)

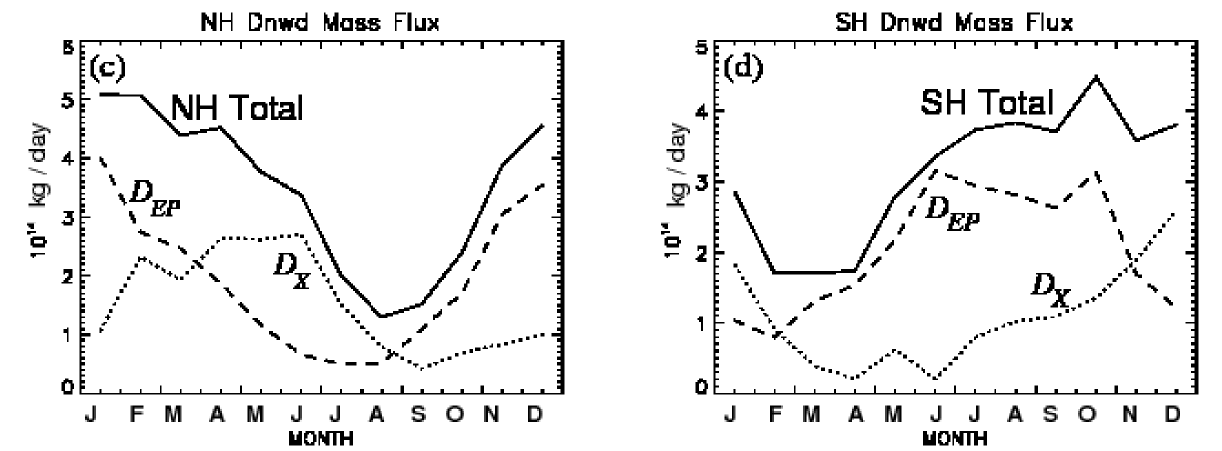
NH Dnwd Mass Flux
(c)
NH Total
$D_{EP}$
$D_X$
$10^{14}$ kg / day
0
1
2
3
4
5
6
J F M A M J J A S O N D
MONTH
SH Dnwd Mass Flux
(d)
SH Total
$D_{EP}$
$D_X$
$10^{14}$ kg / day
0
1
2
3
4
5
J F M A M J J A S O N D
MONTH

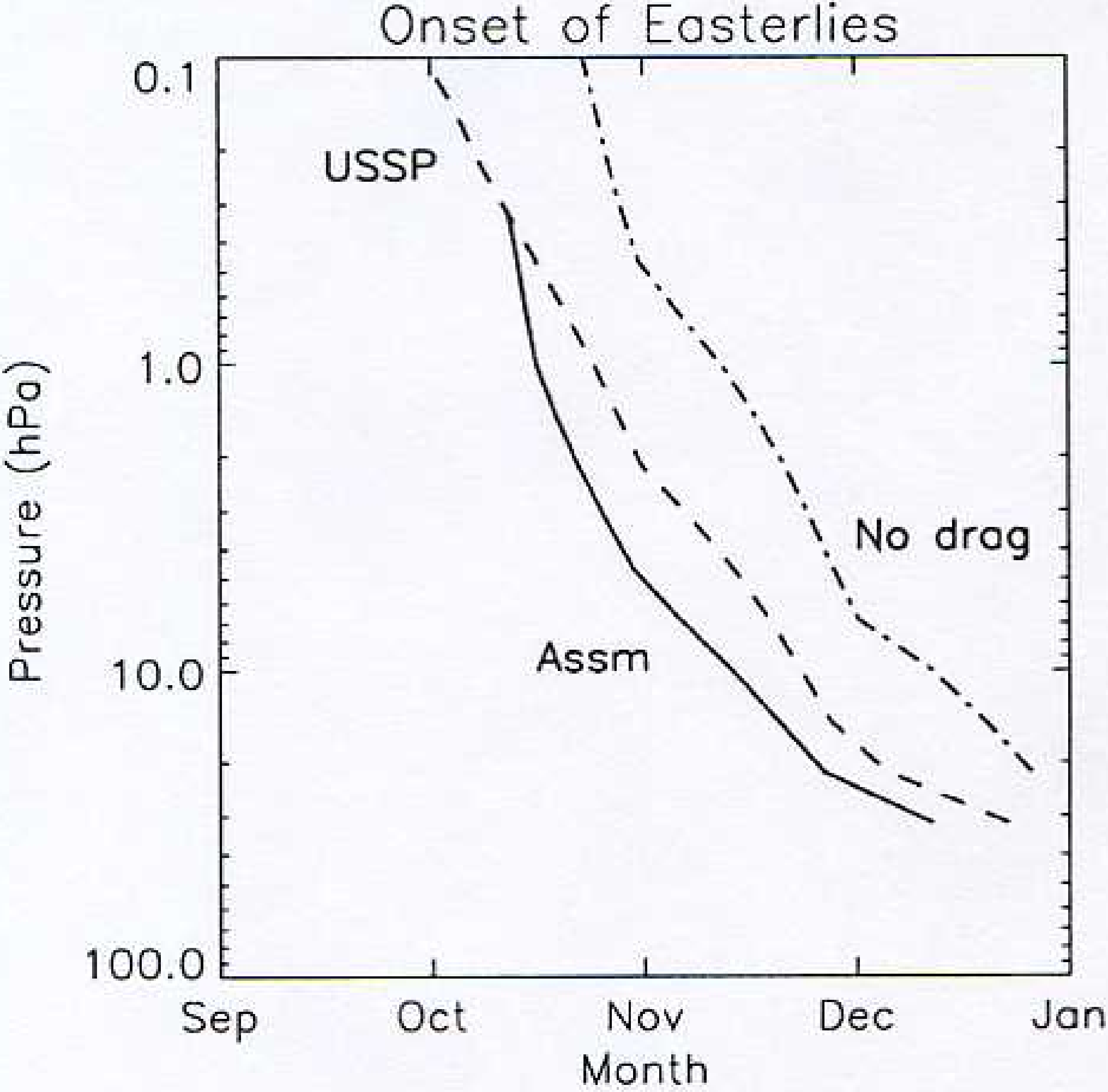

Onset of Easterlies
Pressure (hPa)
0.1
1.0
10.0
100.0
USSP
No drag
Assm
Sep
Oct
Nov
Dec
Jan
Month

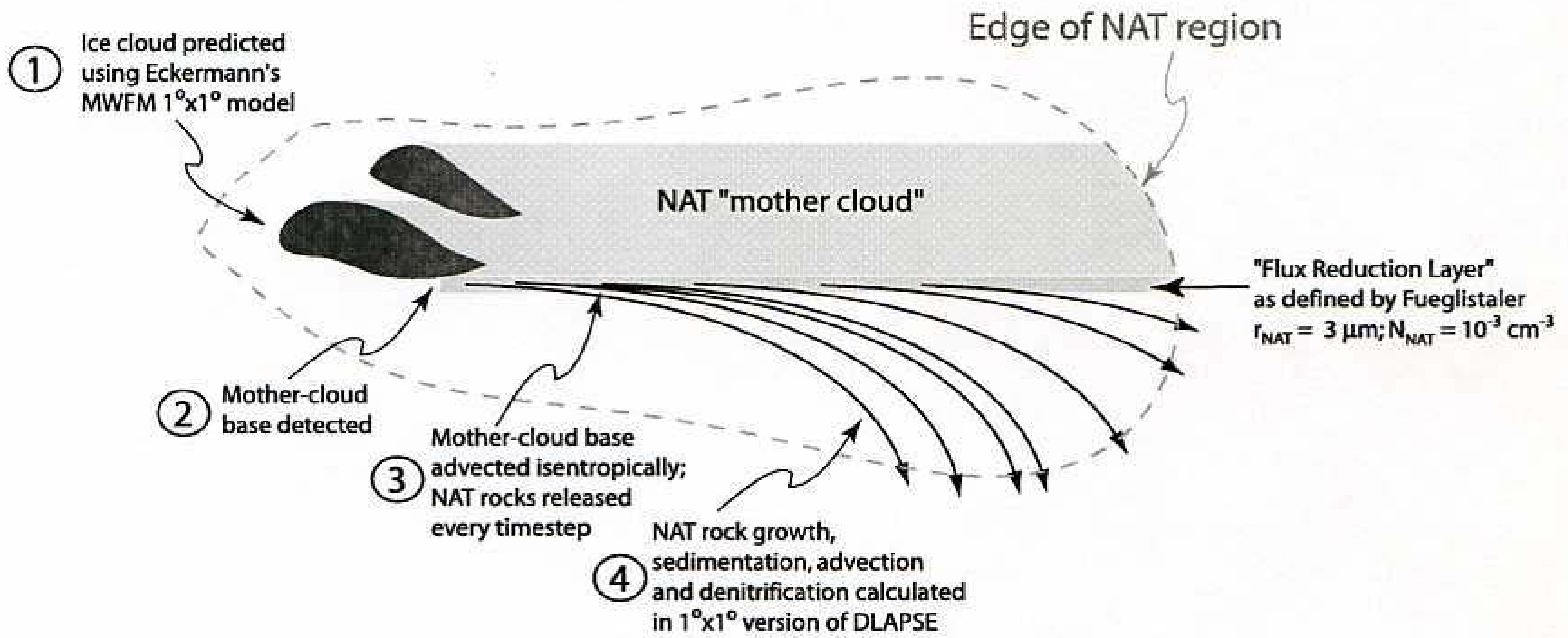

Edge of NAT region
1 Ice cloud predicted using Eckermann's MWFM 1°x1° model
NAT "mother cloud"
"Flux Reduction Layer" as defined by Fueglistaler $r_{NAT} = 3\ \mu m$; $N_{NAT} = 10^{-3}\ cm^{-3}$
2 Mother-cloud base detected
3 Mother-cloud base advected isentropically; NAT rocks released every timestep
4 NAT rock growth, sedimentation, advection and denitrification calculated in 1°x1° version of DLAPSE

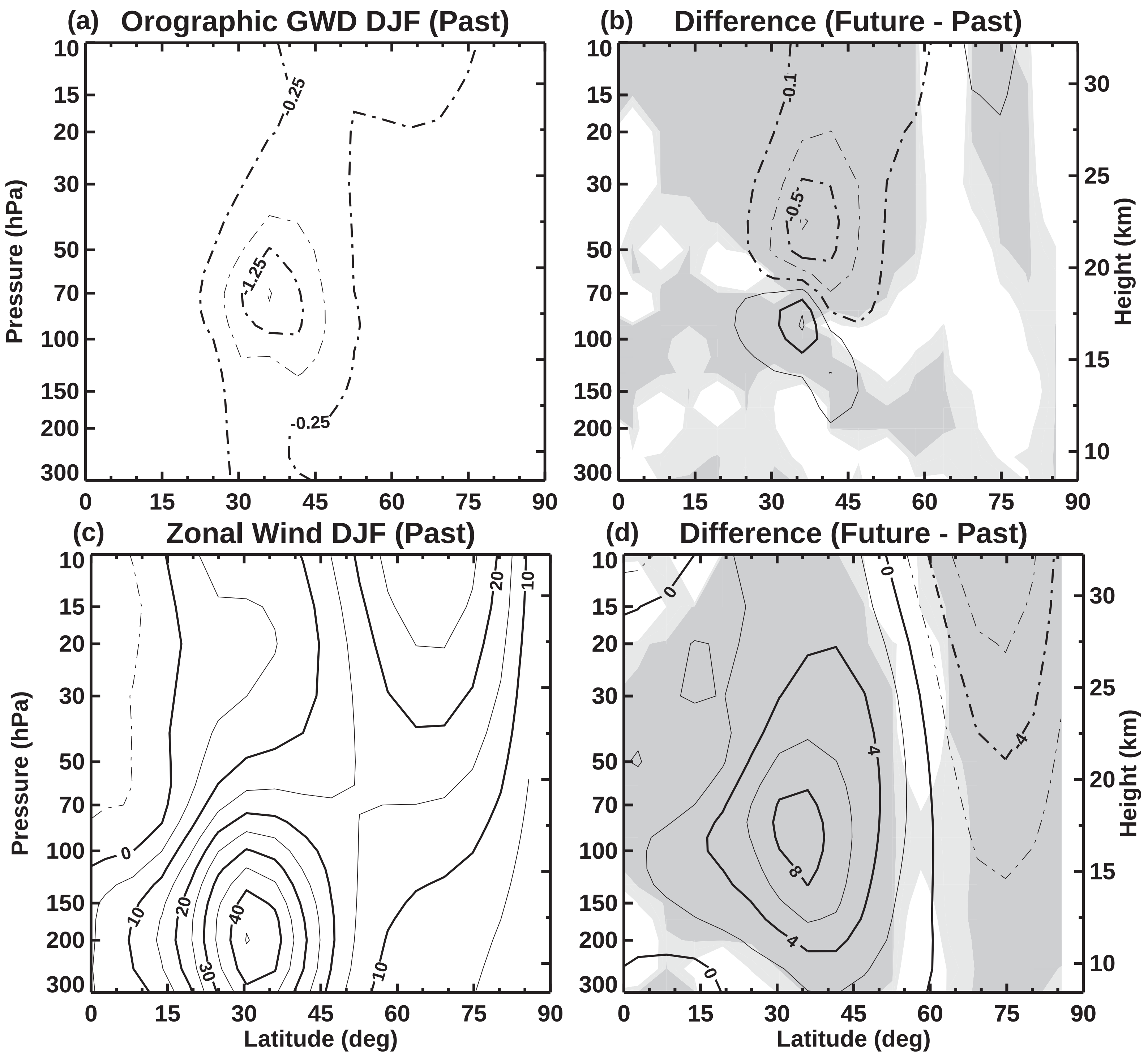
(a) Orographic GWD DJF (Past)
(b) Difference (Future - Past)
(c) Zonal Wind DJF (Past)
(d) Difference (Future - Past)
Pressure (hPa)
Height (km)
Latitude (deg)
-0.25
-1.25
-0.1
-0.5
0
10
20
30
40
-10
4
8
-4

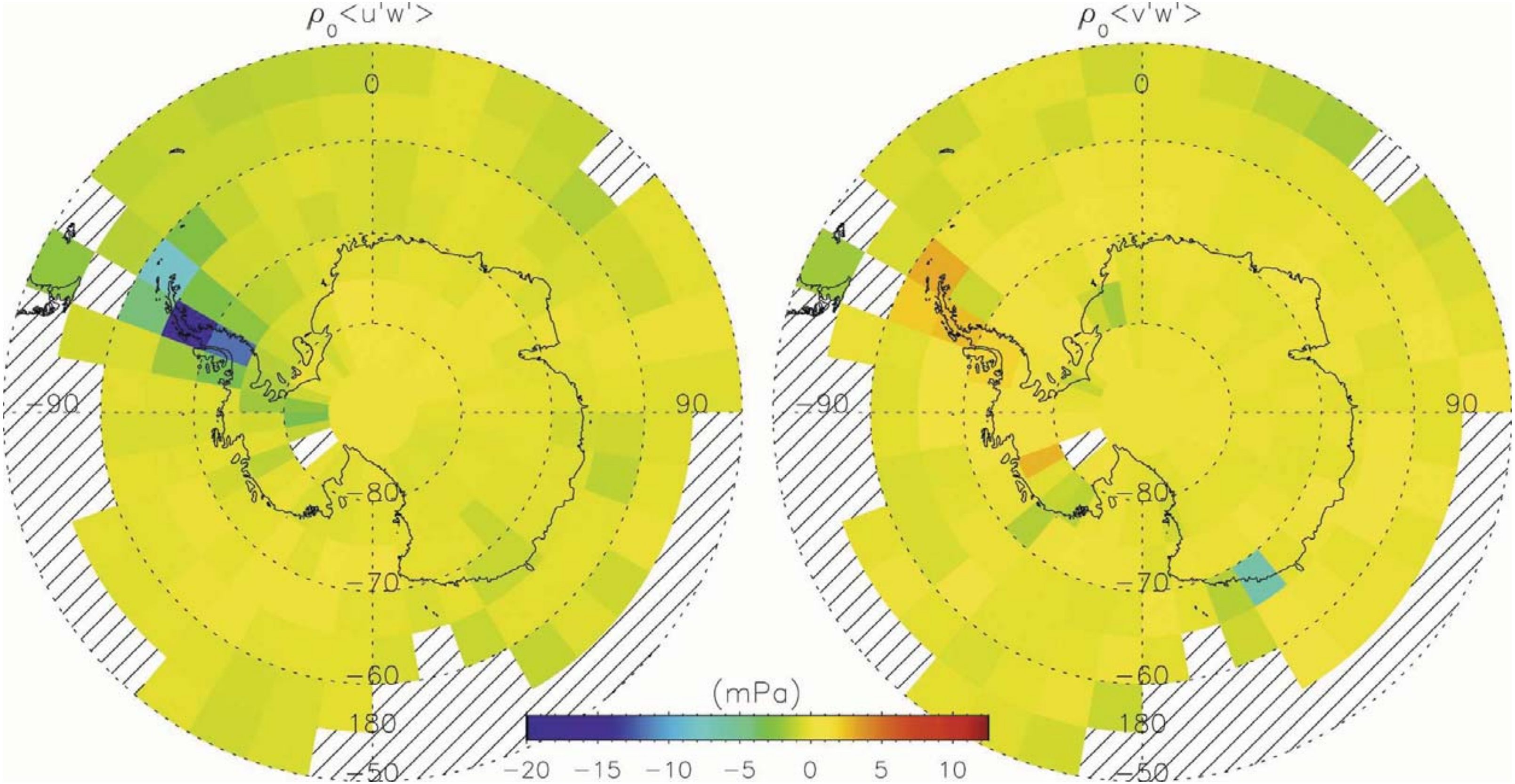

ρ0<u'w'>
ρ0<v'w'>
0
90
−90
180
−80
−70
−60
−50
(mPa)
−20 −15 −10 −5 0 5 10

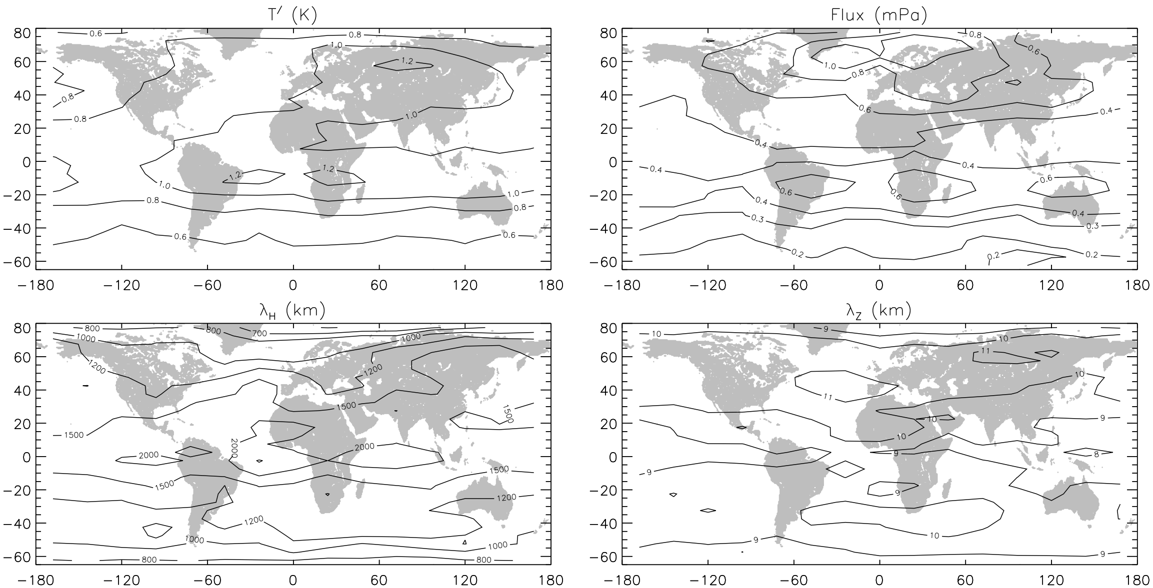

T′ (K)
Flux (mPa)
λ_H (km)
λ_Z (km)
80
60
40
20
0
−20
−40
−60
−180
−120
−60
0
60
120
180

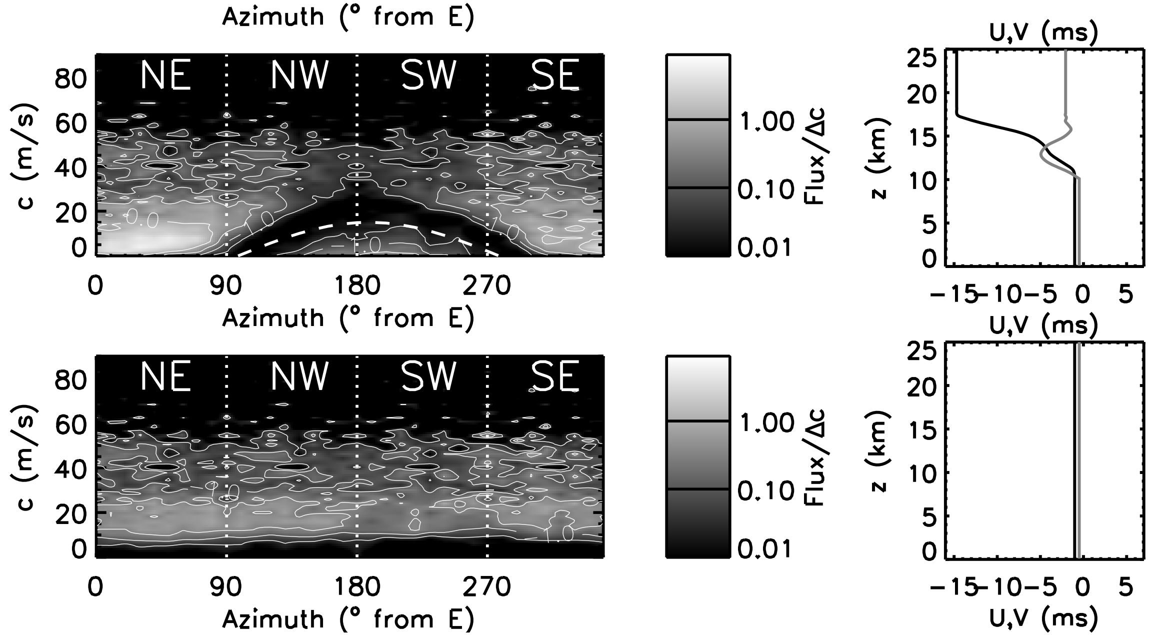
Azimuth (° from E)
NE
NW
SW
SE
c (m/s)
0
20
40
60
80
0
90
180
270
Azimuth (° from E)
1.00
0.10
0.01
Flux/Δc
U,V (ms)
z (km)
0
5
10
15
20
25
−15
−10
−5
0
5
U,V (ms)
NE
NW
SW
SE
c (m/s)
0
20
40
60
80
0
90
180
270
Azimuth (° from E)
1.00
0.10
0.01
Flux/Δc
z (km)
0
5
10
15
20
25
−15
−10
−5
0
5
U,V (ms)

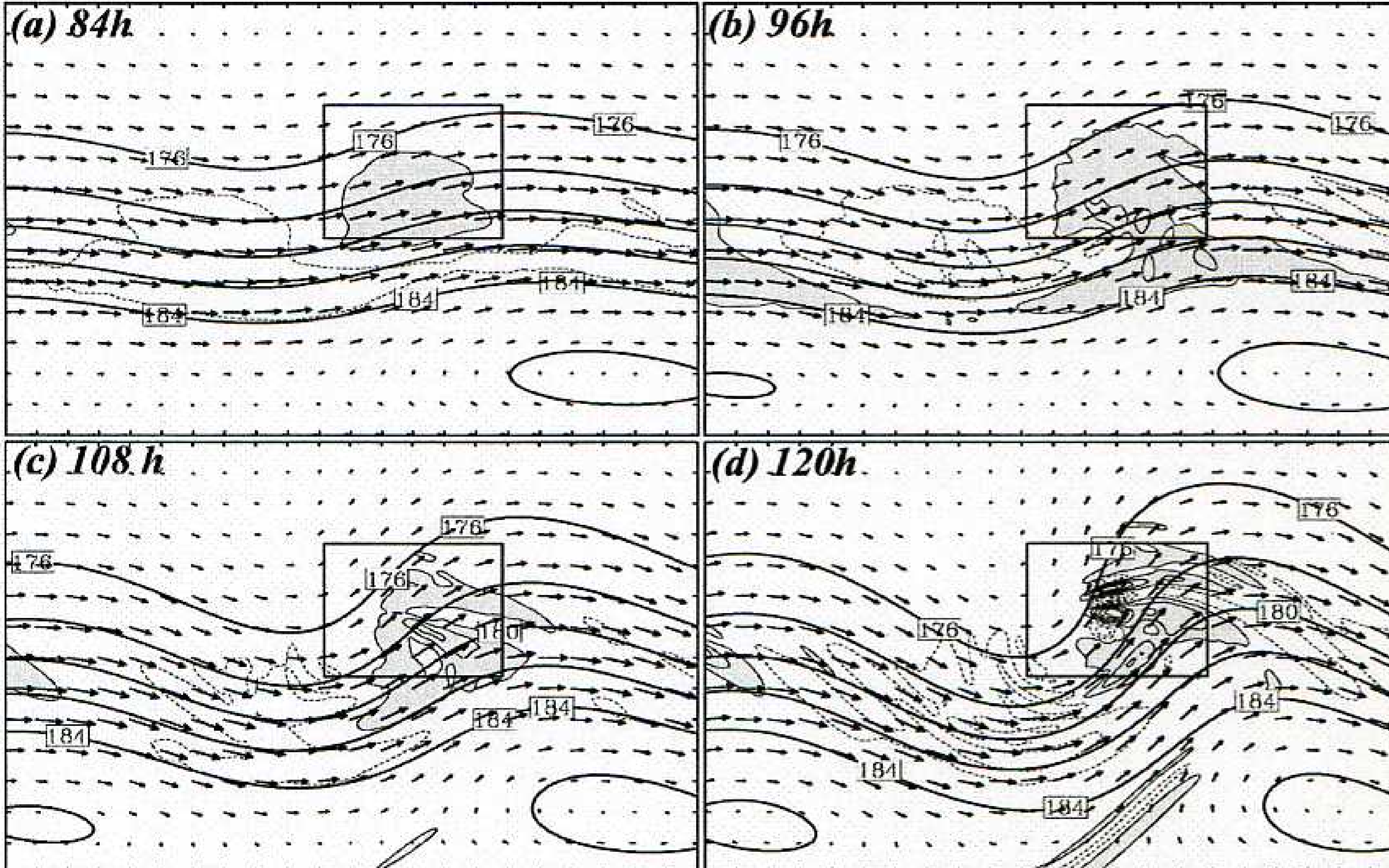

(a) 84h
176
176
176
184
184
184
(b) 96h
176
176
176
184
184
184
(c) 108 h
176
176
176
180
184
184
184
(d) 120h
176
176
176
180
184
184
184